J|A|C|S
ARTICLES
Published on Web 10/12/2002

Fluorescence of *cis*-1-Amino-2-(3-indolyl)cyclohexane-1-carboxylic Acid: A Single Tryptophan χ_1 Rotamer Model

Bo Liu,[†] Reema K. Thalji,[‡] Paul D. Adams,[†] Frank R. Fronczek,[‡] Mark L. McLaughlin,*[,‡] and Mary D. Barkley*[,†]

Contribution from the Department of Chemistry, Case Western Reserve University, Cleveland, Ohio 44106, and Department of Chemistry, Louisiana State University, Baton Rouge, Louisiana 70803

Received July 3, 2001

Abstract: A constrained derivative, *cis*-1-amino-2-(3-indolyl)cyclohexane-1-carboxylic acid, *cis*-W3, was designed to test the rotamer model of tryptophan photophysics. The conformational constraint enforces a single χ_1 conformation, analogous to the $\chi_1 = 60°$ rotamer of tryptophan. The side-chain torsion angles in the X-ray structure of *cis*-W3 were $\chi_1 = 58.5°$ and $\chi_2 = -88.7°$. Molecular mechanics calculations suggested two χ_2 rotamers for *cis*-W3 in solution, $-100°$ and 80°, analogous to the $\chi_2 = \pm 90°$ rotamers of tryptophan. The fluorescence decay of the *cis*-W3 zwitterion was biexponential with lifetimes of 3.1 and 0.3 ns at 25 °C. The relative amplitudes of the lifetime components match the χ_2 rotamer populations predicted by molecular mechanics. The longer lifetime represents the major $\chi_2 = -100°$ rotamer. The shorter lifetime represents the minor $\chi_2 = 80°$ rotamer having the ammonium group closer to C4 of the indole ring (labeled C5 in the *cis*-W3 X-ray structure). Intramolecular excited-state proton transfer occurs at indole C4 in the tryptophan zwitterion (Saito, I.; Sugiyama, H.; Yamamoto, A.; Muramatsu, S.; Matsuura,T. *J. Am. Chem. Soc.* **1984**, *106*, 4286−4287). Photochemical isotope exchange experiments showed that H−D exchange occurs exclusively at C5 in the *cis*-W3 zwitterion, consistent with the presence of the $\chi_2 = 80°$ rotamer in solution. The rates of two nonradiative processes, excited-state proton and electron transfer, were measured for individual χ_2 rotamers. The excited-state proton-transfer rate was determined from H−D exchange and fluorescence lifetime data. The excited-state electron-transfer rate was determined from the temperature dependence of the fluorescence lifetime. The major quenching process in the $-100°$ rotamer is electron transfer from the excited indole to carboxylate. Electron transfer also occurs in the 80° rotamer, but the major quenching process is intramolecular proton transfer. Both quenching processes are suppressed by deprotonation of the amino group. The results for *cis*-W3 provide compelling evidence that the complex fluorescence decay of the tryptophan zwitterion originates in ground-state heterogeneity with the different lifetimes primarily reflecting different intramolecular excited-state proton- and electron-transfer rates in various rotamers.

The complex photophysics of tryptophan is both a blessing and a curse. On one hand, the fluorescence quantum yield and lifetime are highly sensitive to the environment. On the other hand, this very sensitivity hampers the use of protein fluorescence as a structural tool. Despite two decades of work by many investigators, the heterogeneous fluorescence decays of single tryptophans in peptides and proteins remain largely uninterpretable. Even the biexponential fluorescence decay of tryptophan zwitterion is not fully understood. Over the years, several explanations have been advanced to account for the lifetime heterogeneity. Although the origin of the multiexponential decays of proteins remains elusive,[1] the rotamer model has prevailed for simple tryptophan derivatives in aqueous solution.[2,3] According to the rotamer model, multiple fluorescence lifetimes originate from ground-state rotamers about the $C_\alpha-C_\beta$ (χ_1) and $C_\beta-C_\gamma$ (χ_2) bonds of the tryptophan side chain. Presumably, differences in proximity of the indole ring to substituents that quench the fluorescence cause lifetime differences among rotamers. Lifetime measurements in supersonic jets have demonstrated that individual conformers have monoexponential fluorescence decays.[4,5] Tryptophan has six preferred rotamers: three χ_1 rotamers, $\pm 60°$ and 180°, each with two χ_2 rotamers, $\pm 90°$. NMR[6] and molecular modeling[7,8] indicate that all of them exist in solution. Inspection of the structures of

* To whom correspondence should be addressed at CWRU or LSU. CWRU Fax: 216-368-0604. E-mail: mdb4@po.cwru.edu. LSU Fax: 225-388-3458. E-mail: mmclaugh@lsu.edu.
[†] Case Western Reserve University.
[‡] Louisiana State University.

(1) Lakowicz, J. R. *Photochem. Photobiol.* **2000**, *72*, 421−437.
(2) Donzel, B.; Gauduchon, P.; Wahl, P. *J. Am. Chem. Soc.* **1974**, *96*, 801−808.
(3) Szabo, A. G.; Rayner, D. M. *J. Am. Chem. Soc.* **1980**, *102*, 554−563.
(4) Sipior, J.; Sulkes, M.; Auerbach, R.; Boivineau, M. *J. Phys. Chem.* **1987**, *91*, 2016−2018.
(5) Philips, L. A.; Webb, S. P.; Martinez, S. J., III; Fleming, G. R.; Levy, D. H. *J. Am. Chem. Soc.* **1988**, *110*, 1352−1355.

individual rotamers reveals differences in proximity of the indole ring to the ammonium and carboxylate groups. Moreover, there is compelling evidence for several excited-state reactions in the tryptophan zwitterion, including proton transfer,[9] electron transfer,[10,11] and rotamer interconversion.[12] However, several questions still await more straightforward answers. Why do the six rotamers have only two fluorescence lifetimes? What are the lifetimes of individual rotamers? Also, what quenching mechanisms govern those lifetimes?

The indole chromophore has multiple nonradiative decay pathways that compete with emission for deactivation of the excited electronic state and thereby quench the fluorescence. Our previous work on simple indole and constrained tryptophan derivatives dissected the different nonradiative pathways by measuring individual rates.[13−17] The total nonradiative rate k_{nr} is

$$k_{nr} = k_{isc} + k_{si} + k_{pt} + k_{et} \quad (1)$$

Intersystem crossing to the triplet state is independent of temperature and environment in aqueous solution. The intersystem crossing rate k_{isc} is determined from triplet yield and fluorescence lifetime measurements.[16] Solvent quenching refers to the major temperature-dependent nonradiative process that occurs in all indoles in protic solvent and causes a solvent isotope effect on the fluorescence quantum yield and lifetime of simple indoles. The solvent quenching rate k_{si} is obtained from the temperature dependence of the fluorescence lifetime.[13,15] Excited-state exchange of aromatic protons at indole C2, C4, and C7 occurs at neutral pH in the presence of a good proton donor, such as ammonium.[9,14] The proton-transfer rate k_{pt} is measured in photochemical isotope exchange experiments monitored by NMR or mass spectrometry.[17,18] Electron transfer from excited indole to electrophilic acceptors is probably the most important quenching mechanism in proteins. The electron-transfer rate k_{et} can be extracted from the temperature dependence of the fluorescence lifetime.[16,17]

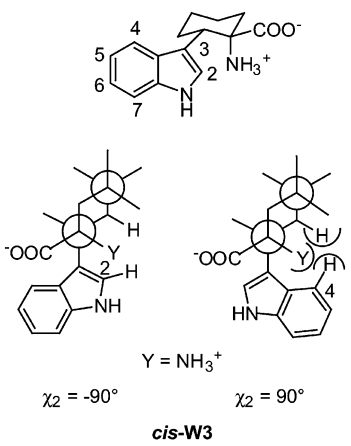

***cis*-W3**

Our strategy for testing the rotamer model is to reduce the number of conformational degrees of freedom. Previously, we studied tetrahydrocarbazoles, which contain 2,3-disubstituted indoles and thereby limit comparison with tryptophan. Here we present a second generation constrained tryptophan, *cis*-1-amino-2-(3-indolyl)cyclohexane-1-carboxylic acid, *cis*-W3, which closely mimics the $\chi_1 = 60°$ rotamer of tryptophan. With a judiciously located six-member ring, a single conformation of the $C_\alpha-C_\beta$ bond of tryptophan is dictated by equatorial placement of the sterically bulky 3-indolyl substituent. Steric hindrance between the amino group and protons on the benzene and cyclohexane rings in the $\chi_2 = 90°$ rotamer (indicated by half-circles) strongly favors the $\chi_2 = -90°$ rotamer. Ground-state conformation is determined by X-ray crystallograpy and molecular modeling. Excited-state properties are determined by steady-state and time-resolved fluorescence techniques and photochemical isotope exchange experiments. The implications of our results for tryptophan photophysics are discussed.

Experimental Section

Synthesis. 2-(3-Indolyl)cyclohexanone. Glacial acetic acid (50 mL) and 2 N H_3PO_4 (13 mL) were heated to 135−140 °C, indole (7 g, 0.06 mol; 99%, Aldrich) and (±)-2-hydroxycyclohexanone dimer (10 g, 0.8 mol; Aldrich) were added, and the mixture was refluxed for 30 min. The mixture was cooled in an ice bath and then poured into 150 mL of ice-cold concentrated ammonium hydroxide with vigorous stirring. The yellow precipitate was collected by filtration and extracted with ethyl acetate. The organic phase was washed, dried, and evaporated to dryness. The gooey residue was dissolved in a small volume of CH_2Cl_2, applied to a silica gel column, and eluted with CH_2Cl_2/ethyl acetate (19:1 vol/vol). After removal of solvent, a light brown solid was obtained (4.3 g, 48% yield). ^{1}H NMR (200 MHz, $CDCl_3$): δ 8.11 (br s, 1H), 7.46 (d, $J = 6.0$ Hz, 1H), 7.35 (d, $J = 6.0$ Hz, 1H), 7.21−7.08 (3H), 3.97−3.92 (dd, $J = 12$, 6 Hz, 1H), 2.65−1.83 (8H). EI-MS: calcd for $C_{14}H_{15}NO$ 213.1154, found 213.1152.

2-(3-Indolyl)cyclohexanespiro-5′-hydantoin. 2-(3-Indolyl)cyclohexanone (2.8 g, 13 mmol) was dissolved in 30 mL of warm methanol, and $(NH_4)_2CO_3$ (3.0 g, 31 mmol) was added. NaCN (3.0 g, 61 mmol; 99.99%, Aldrich) dissolved in 35 mL of water was added dropwise to the mixture in 30 min. Another 3.0 g of $(NH_4)_2CO_3$ was added, and the suspension was stirred at 67 °C for 48 h. The final mixture containing a light yellow precipitate was poured into 250 mL of water, and the pH was adjusted to 7.0 with 6 N HCl. The solution was cooled to 0 °C. The white crystalline precipitate was filtered, washed with a small amount of water, and dried at 80 °C for 3 h (4.32 g, 104% yield; 96% yield after correction for waters of hydration[19]): mp 159−160 °C. IR ν_{max}(KBr): 1724, 1759 (C=O). ^{1}H NMR (250 MHz, DMSO-d_6): δ 10.88 (s, 1H), 10.01 (s, 1H), 8.50 (s, 1H), 7.52 (d, $J = 7.5$ Hz, 1H), 7.27 (d, $J = 7.5$ Hz, 1H), 7.09 (s, 1H), 7.00 (t, $J = 7.5$ Hz, 1H), 6.90 (t, $J = 7.5$ Hz, 1H), 3.34 (dd, $J = 12$, 4 Hz, 1H), 1.99−1.42 (8H). ^{13}C NMR (62.5 MHz, DMSO-d_6): δ 177.72, 156.92, 135.33,

(6) Dezube, B.; Dobson, C. M.; Teague, C. E. *J. Chem. Soc., Perkins Trans. 2* **1981**, 730−735.
(7) Engh, R. A.; Chen, L. X. Q.; Fleming, G. R. *Chem. Phys. Lett.* **1986**, *126*, 365−372.
(8) Gordon, H. L.; Jarrell, H. C.; Szabo, A. G.; Willis, K. J.; Somorjai, R. L. *J. Phys. Chem.* **1992**, *96*, 1915−1921.
(9) Saito, I.; Sugiyama, H.; Yamamoto, A.; Muramatsu, S.; Matsuura, T. *J. Am. Chem. Soc.* **1984**, *106*, 4286−4287.
(10) Chang, M. C.; Petrich, J. W.; McDonald, D. B.; Fleming, G. R. *J. Am. Chem. Soc.* **1983**, *105*, 3819−3824.
(11) Petrich, J. W.; Chang, M. C.; McDonald, D. B.; Fleming, G. R. *J. Am. Chem. Soc.* **1983**, *105*, 3824−3832.
(12) Willis, K. J.; Szabo, A. G.; Kracjarski, D. T. *Chem. Phys. Lett.* **1991**, *182*, 614−616.
(13) McMahon, L. P.; Colucci, W. J.; McLaughlin, M. L.; Barkley, M. D. *J. Am. Chem. Soc.* **1992**, *114*, 8442−8448.
(14) Yu, H.-T.; Colucci, W. J.; McLaughlin, M. L.; Barkley, M. D. *J. Am. Chem. Soc.* **1992**, *114*, 8449−8454.
(15) Yu, H.-T.; Vela, M. A.; Fronczek, F. R.; McLaughlin, M. L.; Barkley, M. D. *J. Am. Chem. Soc.* **1995**, *117*, 348−357.
(16) Chen, Y.; Liu, B.; Yu, H.-T.; Barkley, M. D. *J. Am. Chem. Soc.* **1996**, *118*, 9271−9278.
(17) Chen, Y.; Barkley, M. D. *Biochemistry* **1998**, *37*, 9976−9982.
(18) Shizuka, J.; Serizawa, M.; Kobayashi, J.; Kameta, K.; Sugiyama, H.; Matsuura, T.; Saito, I. *J. Am. Chem. Soc.* **1988**, *110*, 1726−1732.
(19) Gauthier, T. J.; Yokum, T. S.; Morales, G. A.; McLaughlin, M. L.; Liu, Y.-H.; Fronczek, F. R. *Acta Crystallogr.* **1997**, *C53*, 1659−1662.

126.66, 122.84, 120.59, 118.89, 118.02, 113.78, 110.98, 66.11, 38.71, 34.22, 29.39, 25.70, 20.71. EI-MS: calcd for $C_{16}H_{17}N_3O_2$ 283.1321, found 283.1321.

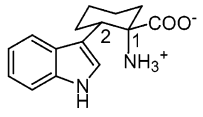

cis-W3

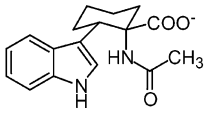

cis-*N*-acetyl-W3

***cis*-1-Amino-2-(3-indolyl)-cyclohexane-1-carboxylic Acid, *cis*-W3.** 2-(3-Indolyl)cyclohexanespiro-5′-hydantoin (250 mg, 0.88 mmol) and $Ba(OH)_2 \cdot 8H_2O$ (16 g) were dissolved in 125 mL of water by heating for 2 h at 80 °C in a 500 mL Parr high-pressure bomb. The solution was purged for 15 min with argon, and the bomb was sealed and placed in a sand bath at 230 °C for 4 days. The temperature was lowered to 80 °C, and $(NH_4)_2CO_3$ (8.0 g) was added to the solution with stirring for 1 h. The solution was clarified by filtration and concentrated to about 10 mL under reduced pressure at 70 °C. The light yellow crystalline product was filtered, washed with 2 mL of water, and dried under vacuum (106 mg, 58% yield): mp 305−307 °C. *cis*-W3 was recrystallized twice from water. ^{1}H NMR (300 MHz, DMSO-d_6): δ 10.91 (s, 1H), 7.71 (d, J = 6.0 Hz, 1H), 7.25 (d, J = 6.0 Hz, 1H), 7.14 (s, 1H), 6.99 (t, J = 6.0 Hz, 1H), 6.87 (t, J = 6.0 Hz, 1H), 7.50−7.2 (br s, 3H), 3.53 (dd, J = 13.5, 3.5 Hz, 1H), 2.15−1.90 (2H), 1.90−1.79 (2H), 1.70−1.52 (2H), 1.52−1.35 (2H). ^{13}C NMR (75 MHz, DMSO-d_6): δ 172.68, 135.72, 127.22, 123.04, 120.58, 120.27, 117.87, 114.73, 110.65, 63.06, 38.18, 33.61, 28.58, 26.05, 20.67. FAB-MS: calcd for $C_{15}H_{19}N_2O_2^+$ (MH^+) 259.1447, found 259.1447.

***cis*-*N*-Acetyl-1-amino-2-(3-indolyl)-cyclohexane-1-carboxylic Acid, *cis*-*N*-Acetyl-W3.** *cis*-W3 (70 mg) was dissolved in 1 mL of 2 N NaOH in an ice bath, and 0.25 mL of acetic anhydride and 4.5 mL of 2 N NaOH were added dropwise in 15 min. The resulting solution was stirred at room temperature for 30 min, and the pH was adjusted to 5 by addition of acetic anhydride. The white precipitate was filtered and washed with 10 mL of water (39 mg, 55% yield): mp 237−238 °C. *cis*-*N*-Acetyl-W3 was crystallized from methanol/water. ^{1}H NMR (300 MHz, DMSO-d_6): δ 11.8 (br s, 1H), 10.9 (s, 1H), 7.51 (s, 1H), 7.44 (d, J = 7.8 Hz, 1H), 7.29 (d, J = 8.1 Hz, 1H), 7.02 (t, J = 7.1 Hz, 1H), 6.91 (t, J = 7.5 Hz, 1H), 6.81 (s, 1H), 2.7 (d, J = 12 Hz, 1H), 2.2−1.2 (12H). ^{13}C NMR (75 MHz, DMSO-d_6): δ 173.9, 169.0, 135.4, 127.4, 123.0, 120.6, 118.4, 118.1, 114.6, 111.1, 61.9, 30.4, 28.6, 25.4, 23.0, 20.6. EI-MS: calcd for $C_{17}H_{20}N_2O_3$ 300.1473, found 300.1480.

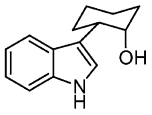

cis-3-InChOH

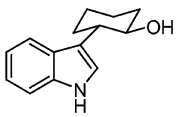

trans-3-InChOH

cis- and *trans*-2-(3-Indolyl)cyclohexanol, *cis*- and *trans*-3-InChOH, were synthesized as described previously.[20] The product was a mixture of *cis*- and *trans*-isomers of 2-(3-indolyl)cyclohexanol (0.7 g, 87% yield). The isomeric mixture was dissolved in a small volume of chloroform, loaded onto a silica gel column, and eluted with 1% methanol in chloroform. Fractions were collected and monitored by TLC. The R_f values of the *cis*- and *trans*-isomers are 0.24 and 0.19. Fractions were pooled and evaporated to dryness. *cis*-Isomer (0.4 g) was crystallized from benzene/petroleum ether (0.2 g, 17% yield): mp = 109−110 °C. ^{1}H NMR (300 MHz, $CDCl_3$): δ 8.08 (br s, 1H), 7.65 (d, J = 9.0 Hz, 1H), 7.40 (d, J = 9.0 Hz, 1H), 7.23 (t, J = 7.5 Hz, 1H), 7.13 (t, J = 8.0 Hz, 1H), 7.10 (s, 1H), 4.21 (s, 1H), 3.16 (dd, J = 12, 4 Hz, 1H), 2.06−1.42 (9H). EI-MS: calcd for $C_{14}H_{17}NO$ 215.1311, found 215.1314. *trans*-Isomer (0.3 g) was crystallized twice from benzene/petroleum ether (0.15 g, 13% yield): mp = 156−157 °C. ^{1}H NMR (300 MHz, $CDCl_3$): δ 8.10 (br s, 1H), 7.75 (d, J = 7.5 Hz, 1H), 7.40 (d, J = 8.0 Hz, 1H), 7.23 (t, J = 7.5 Hz, 1H), 7.14 (t, J = 7.5 Hz, 1H), 7.11 (s, 1H), 3.80−3.77 (1H), 2.82−2.75 (1H), 2.19−1.37 (9H). EI-MS: calcd for $C_{14}H_{17}NO$ 215.1311, found 215.1319.

X-ray Diffraction. X-ray diffraction data were collected on an Enraf-Nonius CAD4 diffractometer using Cu Kα radiation (λ = 1.54184 Å) and a graphite monochromator. Crystal data: $C_{15}H_{20}N_2O_2 \cdot H_2O$, FW = 276.3; orthorhombic space group $P2_12_12_1$; a = 10.1293(6), b = 10.428(1), c = 13.195(1) Å; V = 1393.8(3) Å^3; Z = 4; D_c = 1.317 mg m^{-3}; T = 299 K. Data reduction included corrections for background, Lorentz, polarization, and absorption. Absorption corrections were based on ψ scans. The structure was solved by direct methods and refined using the MolEN programs.[21] Refinement was by full-matrix least squares, with neutral-atom scattering factors and anomalous dispersion corrections. Weights were $w = 4F_o^2[\sigma^2(I) + (0.02F_o^2)^2]^{-1}$. All non-hydrogen atoms were refined anisotropically. Hydrogen atoms were refined isotropically. At convergence, R = 0.030 for 262 parameters and 2733 observed data.

Molecular Mechanics. Calculations were done on a Silicon Graphics INDY workstation using the Discover module of InsightII (Molecular Simulations, Inc.) with the CVFF force field, cross and Morse potential terms, and the dielectric constant of water at 25 °C, ϵ = 78.3. Starting structures for the calculations were based on the X-ray structure of *cis*-W3. The carboxylate was rotated to different positions by changing the ψ torsion angle N2−C14−C15−O2 from 0 to 360° at 15° intervals. For each ψ angle, torsional barriers for χ_2 rotamers were determined by driving the χ_2 torsion angle C14−C9−C7−C6 at 5° intervals and constraining it during energy minimization. *cis*-*N*-Acetyl-W3 was constructed from the *cis*-W3 zwitterion in the Builder module by removing two H's from N2, adding an aldehyde fragment to N2 and a methyl fragment to the aldehyde, and defining the N2−C(carbonyl) bond as a trans peptide bond. The *N*-acetyl group was rotated to different positions by changing the ϕ torsion angle C(carbonyl)−N2−C14−C15 from 0 to 360° at 15° intervals. For each ϕ angle, χ_2 torsional barriers were determined as described above. Rotamer populations were calculated from a Boltzmann distribution of the relative enthalpy at 298 K.

Nuclear Magnetic Resonance. NOESY experiment was performed on a Varian Unity-plus 600 MHz NMR spectrometer at ambient temperature. Ten milligrams of *cis*-W3 was dissolved in 0.6 mL of D_2O. The pD was adjusted to 11.0 with NaOD (99+% D, Aldrich). The HDO signal was suppressed by rf saturation. Acquisition parameters were 6000 Hz (10 ppm) spectral width, 2048 and 256 points in D1 and D2 dimensions (eight scans each), 600 ms mixing time. NMR data were processed using Felix 95.0 (Molecular Simulations, Inc.). Chemical shifts were referenced to the HDO signal taken as 4.80 ppm. A sinebell squared apodization function was used in both D1 and D2 dimensions.

Absorbance and Steady-State Fluorescence. Absorbance was measured on a Cary 3E UV−vis spectrophotometer. The pK of *cis*-W3 was determined from the absorbance change at 270 nm.[22] Sample absorbance was adjusted to <0.1 at 280 nm for steady-state fluorescence measurements and <0.2 at 290 nm for time-resolved fluorescence measurements. *cis*-W3 samples were prepared in 0.01 M phosphate buffer at the indicated pH(D).

Steady-state fluorescence was measured on an SLM 8000 spectrofluorometer with single excitation and emission monochromators as described elsewhere.[13] Fluorescence quantum yields Φ_F were determined at 280 nm excitation wavelength, 25 °C, using a value of 0.14 for tryptophan (Sigma, recrystallized four times from 70% ethanol) in water.[23]

(20) Freter, K. *Liebigs Ann. Chem.* **1978**, 1357−1364.
(21) Fair, C. K. *MolEN, An Interactive Structure Solution Procedure*; Delft: The Netherlands, 1990.
(22) Hermans, J.; Donovan, J. W.; Scheraga, H. A. *J. Biol. Chem.* **1960**, *235*, 91−93.
(23) Chen, R. F. *Anal. Lett.* **1967**, *1*, 35−42.

Time-Resolved Fluorescence. Fluorescence decays were measured by time-correlated single photon counting as described elsewhere.[16,17] Fluorescence decays were acquired at 288 or 290 nm excitation wavelength in a PCA3 multichannel analyzer (Oxford Instruments) with sample alternation. A solution of coffee creamer in water was used for the instrumental response. Decay data were acquired in 1024 channels of 5, 9, 25, and 46 ps/channel for *cis*-W3, and 55 and 64 ps/channel for the other indoles. Lifetimes of monoexponential standards were 1.06 ns for *p*-terphenyl (99+%, Eastman Kodak) in ethanol and 2.85−2.90 ns for *N*-acetyltryptophanamide (NATA; 99+%, Sigma) in water at 25 °C.

Decay curves were deconvolved assuming a multiexponential decay

$$I(t) = \sum_i \alpha_i \exp(-t/\tau_i) \quad (2)$$

where α_i and τ_i are the amplitude and lifetime of component i. The goodness of fit was judged by the value of reduced chi-square χ_r^2 and the shape of the autocorrelation function of the weighted residuals. The radiative k_r and total nonradiative k_{nr} rates were calculated from fluorescence quantum yield and lifetime data.

$$\tau^{-1} = k_r + k_{nr} \quad (3)$$

$$k_r = \Phi_F/\tau \quad (4)$$

For multiexponential decays, the average lifetime $\bar{\tau}$ was used in eqs 3 and 4.

$$\bar{\tau} = \sum_i \alpha_i \tau_i / \sum_i \alpha_i \quad (5)$$

Fluorescence decay curves acquired at various temperatures in the range 5−60 °C were deconvolved in a global analysis with the Arrhenius parameters linked[24]

$$I(t) = \alpha \exp[-\{k_0 + A_1 \exp(-E_1^*/RT) + A_2 \exp(-E_2^*/RT)\}t] \quad (6)$$

where k_0 is the temperature-independent rate, A_i and E_i^* are the frequency factor and activation energy of nonradiative process i, R is the gas constant, and T is absolute temperature. For indoles[16]

$$k_0 = k_r + k_{isc} \quad (7)$$

Photochemical Isotope Exchange. A solution of *cis*-W3 in D_2O (1 mg/mL) was prepared by sonication, placed in a 1-cm quartz cell, and irradiated with a 200 W xenon lamp mounted in a LH 150 Spectral Energy housing. A Corning 7-54 filter was used to remove light <260 nm. H−D exchange at aromatic carbons was monitored on a Varian 300 MHz NMR spectrometer. The HDO resonance was suppressed by rf saturation. Assignment of indole protons was taken from the literature.[9]

The reaction quantum yield Φ_R of H−D exchange was determined at 280 nm excitation (8-nm band-pass) by irradiation with the 400 W xenon lamp of the SLM fluorometer. A 1-cm quartz cell was placed in the filter holder at the exit of the excitation monochromator and masked to control illumination volume.

$$\Phi_R = CVfN_A/I_0 \quad (8)$$

C is the concentration of *cis*-W3 in D_2O, V is the volume of solution, f is the fraction of H−D exchange measured by NMR, N_A is Avogadro's number, and I_0 is the incident light intensity measured by ferrioxalate actinometry.[25,26] Irradiation times of 1.5 h were used to give <10% H−D exchange. The fraction of H−D exchange was calculated relative to an unirradiated sample. The yield of deuteron transfer Φ_D was calculated from[18,27]

$$\Phi_D = \Phi_R[(k_H + k_D)/k_H] \quad (9)$$

where $k_{H(D)}$ is the rate constant for C−H(D) bond cleavage.

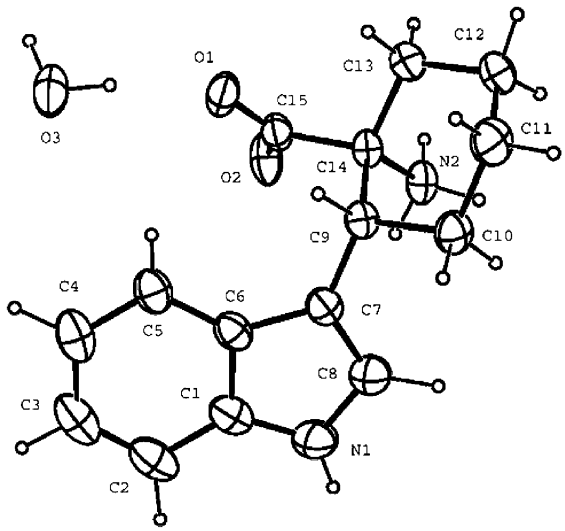

Figure 1. X-ray structure of *cis*-W3 with 40% ellipsoids.

Results and Discussion

Synthesis. Racemic *cis*-W3 is synthesized via a highly diastereoselective Bucherer−Bergs reaction.[28−30] The hydantoin intermediate in the synthesis of *cis*-W3 crystallized as the pure diastereomer.[19] Both *cis*-2-(3-indolyl)cyclohexane-5′-hydantoin and *cis*-W3 give a single spot on TLC and no extraneous peaks in the ^1H and ^{13}C NMR spectra. The other diastereomer, *trans*-W3, has a smaller R_f value and different NMR spectra from *cis*-W3.[31]

X-ray Structure. The racemic sample crystallized as a conglomerate of enantiomerically pure crystals. The absolute structure chosen for X-ray analysis was arbitrary. *cis*-W3 exists as the zwitterion in the monohydrate crystal. The amine N2 is protonated, and the carboxyl group is deprotonated, as evidenced by the C−O distances of 1.242(2) and 1.245(2) Å. The configuration of the zwitterion and the atomic labeling are illustrated in Figure 1. This numbering scheme is used throughout the paper. Both carboxylate O atoms accept intermolecular hydrogen bonds, O1 from the water molecule (O···O 2.6414(14) Å), and O2 from ammonium N2 (N···O 2.7238(14) Å). The cyclohexyl moiety has the chair conformation, with endocyclic torsion angle magnitudes in the range 51.5(1)−56.6(2)°. It is twisted with respect to the indole such that the χ_2 torsion angle C6−C7−C9−C14 is −88.7(1)°. The carboxylate is nearly eclipsed with the ammonium substituent, forming a N2−C14−C15−O2 torsion angle of 8.7(1)°. The χ_1 torsion angle C7−C9−C14−C15 of 58.5(1)° in *cis*-W3 mimics the $\chi_1 = 60°$ rotamer of tryptophan.

Solution Conformation. The conformation of *cis*-W3 in solution was examined by molecular mechanics calculations and

(24) Beechem, J. M. *Chem. Phys. Lipids* **1989**, *50*, 237−251.
(25) Parker, G. A. *Proc. R. Soc. London* **1953**, *A220*, 104−116.
(26) Hatchard, C. G.; Hatchard, C. A. *Proc. R. Soc. London* **1956**, *A235*, 518−536.
(27) Shizuka, H.; Serizawa, M.; Shimo, T.; Saito, I.; Matsuura, T. *J. Am. Chem. Soc.* **1988**, *110*, 1930−1934.
(28) Bucherer, H. T.; Steiner, W. *J. Prakt. Chem.* **1934**, *140*, 291−316.
(29) Bucherer, H. T.; Lieb, V. A. *J. Prakt. Chem.* **1934**, *141*, 5−43.
(30) Lopez, C. A.; Trigo, G. G. *Adv. Heterocycl. Chem.* **1985**, *38*, 177−228.
(31) Liu, B. Ph.D. Thesis, Case Western Reserve University, 1999.

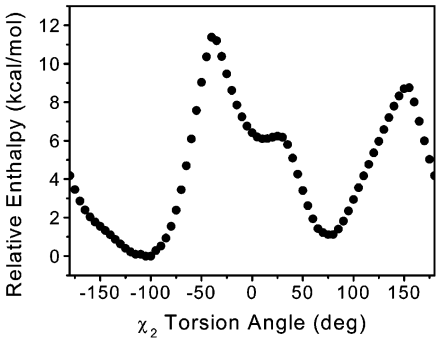

Figure 2. Torsional barriers for χ_2 rotamer interconversion calculated by molecular mechanics.

NMR. Minimum enthalpy conformations of the cyclohexane ring were explored from a variety of starting structures. The chair is the lowest enthalpy conformation, with the boat and twist boat being at least 3 kcal/mol higher. The χ_2 potential surface was obtained by driving the torsion angle C6−C7−C9−C14 (Figure 2). Two minimum enthalpy rotamers at about $\chi_2 = -105$ to $-100°$ and $\chi_2 = 75$ to $80°$ were found for all orientations of carboxylate. The $-100°$ rotamer with $\psi = 4.8°$ represents the global minimum, differing slightly from the crystal structure. The relative enthalpy of the $\chi_2 = 80°$ rotamer is 1.1 kcal/mol. The calculated populations are 0.87 and 0.13 for the $-100°$ and $80°$ rotamers at 25 °C. The lowest torsional barrier between these two rotamers is about 7.6 kcal/mol. The plateau at about $\chi_2 = 10$ to $15°$ represents a rotamer with the indole ring perpendicular to the plane of ammonium, carboxylate, and α-carbon C14. This metastable rotamer is about 5.1 kcal/mol above the global minimum.

The ^{1}H NMR spectrum of *cis*-W3 in D_2O shows the cyclohexane ring in the chair conformation with the indole in the equatorial position. The cyclohexane H9 couples with the adjacent diastereotopic CH_2-10 methylene and appears as a resolved double of doublet with coupling constants J of 12.9 and 4.0 Hz. In cyclohexane rings, coupling constants between axial protons are about 8−14 Hz, whereas coupling constants between axial and equatorial protons are about 2−5 Hz.[32] The calculated torsion angles H9−C9−C10−$H10_e$ and H9−C9−C10−$H10_a$ are 64° and 180°,[33] indicating that the cyclohexane ring is quite rigid. The ^{1}H and ^{13}C NMR spectra at 5 °C show a single set of resonances. If two χ_2 rotamers are present in solution, either the two rotamers interconvert rapidly on the NMR time scale or both proton and carbon chemical shifts are insensitive to environmental differences between rotamers.

A semiquantitative analysis of local NOE intensities suggests that the predominant rotamer in solution is $\chi_2 = -100°$. The NOESY spectrum of *cis*-W3 in D_2O shows a strong NOE between indole H5 and cyclohexane H9 and a weak NOE between indole H8 and H9 (data not shown). According to molecular modeling, the H5 and H9 protons are parallel and 2.6 Å apart in the $\chi_2 = -100°$ rotamer, as compared to perpendicular and 4.1 Å apart in the $\chi_2 = 80°$ rotamer. The H8 and H9 protons are antiparallel and 3.8 Å apart in the $\chi_2 = -100°$ rotamer, but parallel and only 2.8 Å apart in the $\chi_2 = 80°$ rotamer. The about 8-fold higher NOE intensity for H5−H9 than H8−H9 is consistent with $\chi_2 = -100°$ being the major conformation. The weak H8−H9 NOE could arise from one or both χ_2 rotamers. However, the antiparallel orientation of H8 and H9 protons in the $\chi_2 = -100°$ rotamer may give a reduced or even negative NOE.[34] This together with the parallel orientation and 1 Å shorter distance in the $\chi_2 = 80°$ rotamer supports the presence of a minor $\chi_2 = 80°$ conformation.

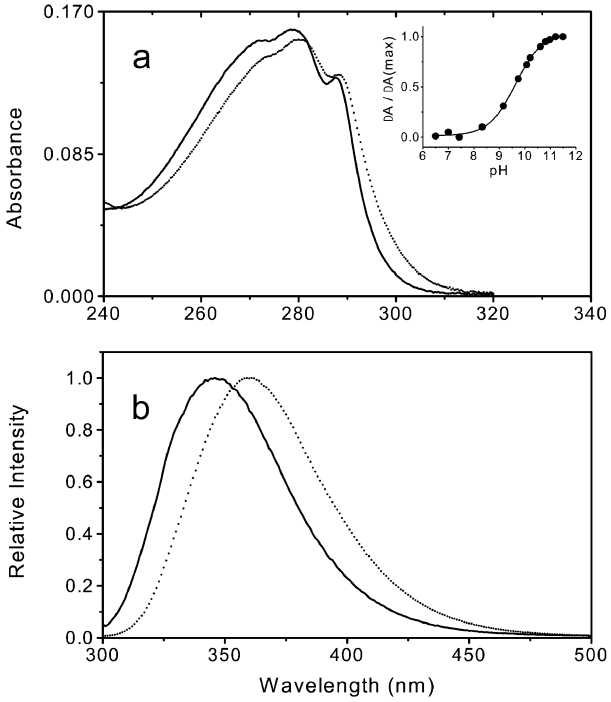

Figure 3. Spectra of the *cis*-W3 (−) zwitterion and (···) anion at 25 °C. (a) Absorption spectra of 2.9×10^{-5} M *cis*-W3 at (−) pH 6.5 and (···) pH 10.6. Inset is a plot of the absorbance change at 270 nm versus pH: $\Delta A = A(\text{pH}) - A(\text{pH } 7.4)$; $\Delta A(\text{max}) = A(\text{pH } 11.5) - A(\text{pH } 7.4)$. (b) Fluorescence emission spectra at 280 nm excitation wavelength at (−) pH 7.0 and (···) pH 10.4.

In *cis*-*N*-acetyl-W3, molecular mechanics calculations identified four minimum enthalpy conformations, the $-100°$ and $80°$ χ_2 rotamers of two backbone torsion angles, $\phi = 60°$ and $\phi = -45°$. The $\phi = 60°$, $\chi_2 = -100°$ conformer represents the global minimum. The relative enthalpies of the other three conformers are about 0.7 kcal/mol. The calculated populations are 0.52 for the $\phi = 60°$, $\chi_2 = -100°$ conformer and 0.16 for each of the others. The torsional barriers for χ_2 rotamer interconversion are higher in the *N*-acetyl derivative (9.1 and 11 kcal/mol in the $\phi = 60°$ and $-45°$ conformers) than in *cis*-W3. The torsional barriers for interconversion between the two ϕ conformers are 4.9 kcal/mol in both χ_2 rotamers.

Absorbance and Steady-State Fluorescence. Figure 3a shows the absorption spectra of the zwitterion and anion of *cis*-W3, which are identical to the spectra of tryptophan. The absorption spectrum shifts about 2 nm to the red upon deprotonation of the ammonium. A p*K* of 9.5 was determined for the amino group of *cis*-W3 from the absorbance change at 270 nm (inset of Figure 3a), in good agreement with the value of 9.4 for tryptophan.[22] These results indicate that the cyclohexane ring in *cis*-W3 does not perturb the electronic energy levels of the indole ring.

(32) Bovey, F. A.; Jelinski, L.; Mirau, P. A. *Nuclear Magnetic Resonance Spectroscopy*, 2nd ed.; Academic Press: San Diego, 1988.
(33) Colucci, W. J.; Jungk, S. J.; Gandour, R. D. *J. Am. Chem. Soc.* **1985**, *107*, 335−343.
(34) Derome, A. E. *Modern NMR Techniques for Chemistry Research*; Pergamon Press: Oxford, 1987; pp 122−124.

Table 1. Quantum Yield and Lifetime Data in H_2O and D_2O, 25 °C[a]

	λ_{max}, nm	Φ_F	τ^b (ns)	k_r (10^7 s^{-1})	k_{nr} (10^7 s^{-1})
			cis-W3		
pH 6.5	346	0.14 ± 0.01	2.7 ± 0.1	5.1 ± 0.4	31 ± 1
pD 7.0	346	0.20 ± 0.01	3.6 ± 0.1	5.6 ± 0.3	22 ± 1
pH 11.2	359	0.32 ± 0.02	6.5 ± 0.1	4.9 ± 0.3	10.5 ± 0.4
pD 12.2	359	0.46 ± 0.02	10.0 ± 0.1	4.6 ± 0.3	5.4 ± 0.4
			cis-*N*-acetyl-W3		
pH 6.0	362	0.31 ± 0.02	7.8 ± 0.1	4.0 ± 0.3	8.8 ± 0.3
pD 6.5	362	0.46 ± 0.02	11.2 ± 0.1	4.1 ± 0.2	4.8 ± 0.3
			tryptophan		
pH 7[c]	352	0.14	2.6	5.4	33
pD 7	352	0.29[d]	5.2[c]	5.6	14
pH 10.5[c]	359	0.31	7.6	4.1	9.1
pD 9.9[e]			9.0		
			N-acetyltryptophan		
pH 7	363[f]	0.21[c]	4.8[c]	4.4	16
pD 7		0.30[d]	5.8[d]	5.2	12
			cis-2-(3-indolyl)cyclohexanol		
pH 6.5	360	0.32 ± 0.01	8.4 ± 0.1	3.8 ± 0.1	8.1 ± 0.2
pD 6.5	360	0.46 ± 0.02	11.8 ± 0.1	3.9 ± 0.2	4.6 ± 0.2
			trans-2-(3-indolyl)cyclohexanol		
pH 7.0	360	0.35 ± 0.02	8.8 ± 0.1	4.0 ± 0.2	7.4 ± 0.2
pD 7.0	360	0.48 ± 0.02	11.8 ± 0.1	4.1 ± 0.2	4.4 ± 0.2
			3-methylindole[g]		
pH 7.0	364	0.34	8.2	4.1	8.1
pD 7.0	364	0.50	12.0	4.2	4.1

[a] Values with standard deviation are from three to five experiments. [b] Average lifetime for biexponential decays. [c] Reference 3 at 20 °C. [d] Reference 37. [e] Reference 51. [f] Reference 40 at 20 °C. [g] Reference 14.

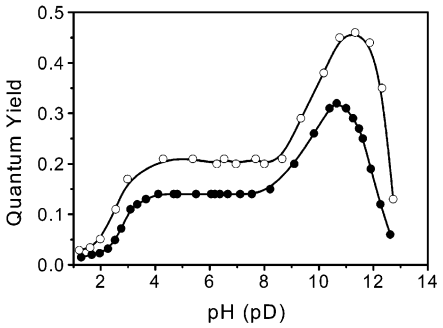

Figure 4. pH dependence of fluorescence quantum yield of *cis*-W3 at 25 °C, 280 nm excitation wavelength: (●) H_2O and (○) D_2O.

Figure 3b shows the emission spectra of the zwitterion and anion of *cis*-W3. The emission spectrum shifts about 13 nm to the red upon deprotonation. The zwitterion emission spectrum is blue shifted about 6 nm in *cis*-W3 as compared to that of tryptophan. The anion emission spectra are identical in *cis*-W3 and tryptophan. The pH dependence of the fluorescence quantum yield of *cis*-W3 in H_2O and D_2O at 25 °C is shown in Figure 4. The pH profiles are similar to those of tryptophan,[35] with large increases in quantum yield upon deprotonation of the ammonium and a deuterium isotope effect throughout the entire pH range. The quantum yield drops at the extremes of pH are due to two excited-state proton-transfer reactions: acid-catalyzed protonation of the indole ring with pK^* ≈ 3 and base-catalyzed deprotonation of the indole nitrogen with pK^* ≈ 12.[36] In tryptophan, the quenching process at intermediate pH is due to a regioselective intramolecular excited-state proton transfer catalyzed by the ammonium.[9] The deuterium isotope effect comprises contributions from water quenching and excited-state proton transfer.[13,14] The deuterium isotope effect at intermediate pH is smaller in *cis*-W3 than in tryptophan. The ratio of quantum yields in D_2O to H_2O is only 1.4 for the *cis*-W3 zwitterion as compared to 2.1 for the tryptophan zwitterion (Table 1).

Blocking the amino group of *cis*-W3 by acetylation increases the quantum yield in H_2O and D_2O over 2-fold to values approaching those of *cis*-W3 anion and 3-methylindole (Table 1). The effect of *N*-acetylation on quantum yield is less pronounced in tryptophan.[3,37] Replacing the amino acid functional groups at the α-carbon C14 by a hydroxyl group cis or trans to the indole ring at the *β*-carbon C9 has similar effects. The quantum yields of *cis*- and *trans*-2-(3-indolyl)cyclohexanol in H_2O and D_2O are very close to those of 3-methylindole.

Time-Resolved Fluorescence. Fluorescence decay data were collected for the constrained tryptophan derivatives in H_2O and D_2O at 25 °C (Table 2). Time-resolved emission spectral data were acquired for the *cis*-W3 zwitterion and *cis*-*N*-acetyl-W3 in H_2O. Decay curves at different emission wavelengths were deconvolved in single curve analyses and in multiple curve analyses with lifetimes but not amplitudes constrained to be the same in all of the curves. The data for the W3 zwitterion in H_2O and D_2O and *cis*-*N*-acetyl-W3 in H_2O were best fit by double exponential functions. The data for *cis*-W3 anion as well as *cis*- and *trans*-2-(3-indolyl)cyclohexanol gave adequate fits to single exponential functions ($\chi_r^2 = 1.2-1.6$).

The *cis*-W3 zwitterion in H_2O at 25 °C has lifetimes of 3.1 and 0.33 ns, very close to the lifetimes of tryptophan at 20 °C.[3] Unlike tryptophan, the amplitudes of the two decays are independent of emission wavelength from 330 to 400 nm, indicating that the two lifetime components have the same emission spectra. The amplitudes of the longer (0.87 and 0.9) and shorter (0.13 and 0.10) lifetime components of the *cis*-W3

(35) Lehrer, S. S. *J. Am. Chem. Soc.* **1970**, *92*, 3459−3462.
(36) Vander Donckt, E. *Bull. Soc. Chim. Belg.* **1969**, *78*, 69−75.
(37) Kirby, E. P.; Steiner, R. F. *J. Phys. Chem.* **1970**, *74*, 4480−4490.

Table 2. Time-Resolved Fluorescence Data in H_2O and D_2O, 25 °C[a]

compound	solvent	α_1 (λ, nm)	τ_1 (ns)	τ_2 (ns)	χ_r^2
cis-W3	pH 6.5[b]	1.0	3.1 ± 0.1		3.6
		0.87 ± 0.02	3.1 ± 0.1	0.33 ± 0.02	1.4
	pD 7.0[b]	1.0	3.9 ± 0.1		2.3
		0.90 ± 0.02	3.9 ± 0.1	0.40 ± 0.02	1.5
	pH 11.2[c]	1.0	6.5		1.6
		0.94	6.6 ± 0.1	1.3 ± 0.1	1.2
	pD 12.2[c]	1.0	10.0 ± 0.1		1.4
cis-*N*-acetyl-W3	pH 6.0[d]	1.0	8.3 ± 0.3		4.3
		0.67 (330)	9.7	5.0	1.6
		0.65 (350)			
		0.55 (370)			
		0.54 (390)			
	pD 6.5[c]	1.0	11.2 ± 0.1		1.6

[a] Values with standard deviations are from three to five experiments. $\sum_i \alpha_i = 1$. [b] Emission wavelength 350 nm. [c] Emission wavelength 370 nm. [d] Global analysis of data acquired at 330−390 nm emission wavelength, 20-nm increments.

zwitterion in H_2O and D_2O correlate well with the ground-state populations of 0.87 and 0.13 of the two χ_2 rotamers of *cis*-W3 determined by molecular modeling. This assigns the longer lifetime component to the major $\chi_2 = -100°$ rotamer and the shorter lifetime component to the minor $\chi_2 = 80°$ rotamer.

cis-*N*-Acetyl-W3 has lifetimes of 9.7 and 5.0 ns with amplitudes of about 0.6 and 0.4 in H_2O at 25 °C. The amplitudes of the biexponential decay depend slightly on emission wavelength. The 9.7-ns lifetime of the major component is close to the value for 3-methylindole, whereas the 5.0-ns lifetime of the minor component is close to the value of *N*-acetyltryptophan (Table 1). The amplitudes of the longer (0.67−0.54) and shorter (0.33−0.46) lifetime components correlate roughly with the ground-state populations of the two ϕ conformers (0.68 for $\phi = 60°$ and 0.32 for $\phi = -45°$) predicted by molecular modeling. The fluorescence decay in D_2O collapses to a single exponential, presumably because the two lifetimes become too close to resolve. Both mono- and biexponential fluorescence decays have been reported for *N*-acetyltryptophan.[3,38−40]

The radiative k_r and total nonradiative k_{nr} rates were calculated from quantum yield and lifetime data according to eqs 3−5. The radiative rates of the *cis*-W3 zwitterion and anion and of *cis*-*N*-acetyl-W3 are independent of solvent isotope within error. The k_r values of *cis*-W3 and tryptophan appear to be about the same. In contrast, the nonradiative rates depend on solvent isotope. As noted above for quantum yields, the deuterium isotope effect on k_{nr} is less in the *cis*-W3 zwitterion than in the tryptophan zwitterion.

Excited-State Proton Transfer. Intermolecular excited-state proton transfer catalyzed by good proton donors, such as the α-ammonium group of amino acid zwitterions, occurs at the C2, C4, and C7 positions of the indole ring in 3-methylindole.[14,41] The corresponding positions in *cis*-W3 are C8, C5, and C2. The sites(s) of intramolecular proton transfer in tryptophan derivatives are governed by stereochemical considerations.[18] Inspection of molecular models shows that the two χ_2 rotamers of *cis*-W3 differ in proximity of the ammonium to

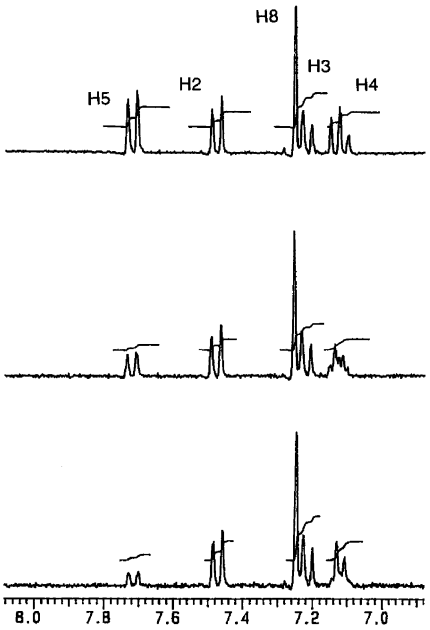

Figure 5. Deuterium incorporation upon irradiation of *cis*-W3 in D_2O. Partial ^1H NMR spectra after (top) 0 h, (middle) 1.5 h, and (bottom) 4.5 h irradiation with a 200 W xenon lamp.

potential proton-transfer sites on the indole ring. The ammonium N2 can come 1.8 Å closer to C5 in the minor 80° rotamer (N···C 3.5 Å) than in the major −100° rotamer (N···C 5.3 Å), and 1.4 Å closer to C8 in the major −100° rotamer (N···C 3.5 Å) than in the minor 80° rotamer (N···C 4.9 Å). Therefore, we expect to observe H−D exchange at both C5 of the minor 80° rotamer and C8 of the major −100° rotamer.

Photochemical H−D exchange experiments were performed on *cis*-W3 in D_2O at pD 6.5 at room temperature. Deuterium incorporation at C5 on the indole ring is apparent in the NMR spectra of irradiated samples (Figure 5). H−D exchange on other aromatic carbons was negligible in samples with up to 67% exchange at C5. The observation of H−D exchange at C5 confirms the presence of the $\chi_2 = 80°$ rotamer in solution, as predicted by molecular modeling. The absence of exchange at C8 indicates that excited-state proton transfer occurs only in the 80° rotamer. The reaction quantum yield $\Phi_R = 0.077 \pm 0.006$ for H−D exchange in D_2O was determined by ferrioxalate actinometry using the total concentration of *cis*-W3 in eq 8. The reaction yield of 80° rotamer is $\Phi_{R2} = 0.59 \pm 0.04$ on the basis of the mole fraction of this rotamer estimated from molecular mechanics calculations. The isotope exchange reaction is proposed to proceed by electrophilic attack of deuteron on aromatic carbon followed by cleavage of the C−H or C−D bond.[42] Loss of a deuteron is not detectable. For photochemical isotope exchange reactions with aryl cation intermediates, $k_H/k_D = 1.7 \pm 0.3$ in 20% acetonitrile solvent. The quantum yield of deuteron transfer in the 80° rotamer is calculated from eq 9. The resulting $\Phi_{D2} = 0.94 \pm 0.07$ is used to calculate the deuteron transfer rate k_{pt}^D of the 80° rotamer from the lifetime in D_2O (Table 2)

$$k_{pt}^{D} = \Phi_{D2}/\tau_2^{D} \qquad (10)$$

giving $k_{pt}^D = (2.3 \pm 0.2) \times 10^9\ s^{-1}$.

(38) Ross, J. B. A.; Rousslang, K. W.; Brand, L. *Biochemistry* **1981**, *20*, 4361−4369.
(39) Privat, J. P.; Wahl, P.; Brochon, J. C. *Biochimie* **1985**, *67*, 949−958.
(40) Eftink, M. R.; Jia, Y.; Hu, D.; Ghiron, C. A. *J. Phys. Chem.* **1995**, *99*, 5713−5723.
(41) Chen, Y.; Liu, B.; Barkley, M. D. *J. Am. Chem. Soc.* **1995**, *117*, 5608−5609.
(42) Shizuka, H.; Tobita, S. *J. Am. Chem. Soc.* **1982**, *104*, 6919−6927.

We can also estimate proton-transfer rates k_{pt} by assuming that the lifetime difference between rotamers in Table 2 is due entirely to excited-state proton transfer.

$$k_{pt} = \tau_2^{-1} - \tau_1^{-1} \quad (11)$$

The lifetime data in D_2O give a deuteron transfer rate $k_{pt}^D = (2.2 \pm 0.1) \times 10^9\ s^{-1}$. The k_{pt}^D values obtained from H−D exchange and fluorescence lifetime data are essentially the same. Estimating the proton transfer rate from lifetime data in H_2O gives $k_{pt}^H = (2.7 \pm 0.2) \times 10^9\ s^{-1}$. The kinetic isotope effect on the regioselective intramolecular exchange reaction catalyzed by the ammonium in *cis*-W3 appears to be only $k_{pt}^H/k_{pt}^D = 1.2$. This value is lower than the 2- to 4-fold isotope effects on intermolecular exchange in 3-methylindole catalyzed by the α-ammonium of glycine, the ϵ-ammonium of lysine, and the phenolic proton of tyrosine.[17]

Excited-State Electron Transfer. The total nonradiative rate k_{nr} is 3- to 4-fold higher in the zwitterions as compared to 3-methylindole and other compounds in Table 1. In the case of *cis*-W3, the 80° rotamer represents about 10% of the population. Proton transfer from the ammonium to C5 in the 80° rotamer lowers the average lifetime about 10% relative to the lifetime of the −100° rotamer and therefore contributes only about 10% to the nonradiative rate of the *cis*-W3 zwitterion calculated from eqs 3 and 5. As noted for the tryptophan zwitterion, there must be another major fluorescence quenching mechanism besides proton transfer.[27] We propose that electron transfer from excited indole to carboxylate is the other major quenching mechanism in the *cis*-W3 zwitterion.[17] Carboxylate does not quench 3-methylindole fluorescence.[16] However, protonated carboxyl is a moderate electron-transfer quencher.[17] Presumably, the carboxylate in *cis*-W3 and the tryptophan zwitterion is activated by the proximal ammonium and becomes a better electron acceptor.[10]

We can use eq 1 to estimate the electron transfer rate in the −100° rotamer, because $k_{pt} = 0$ in this rotamer. Assuming that the intersystem crossing and water quenching rates are roughly the same as they are in tryptophan and NATA[16] and using the values of the radiative rate and τ_1 for the *cis*-W3 zwitterion in Tables 1 and 2, eqs 1 and 3 give $k_{et} = 1.9 \times 10^8\ s^{-1}$ for the −100° rotamer at 25 °C in H_2O.

In favorable cases, the electron-transfer rate can be measured directly from the temperature dependence of the fluorescence lifetime.[16]

$$\tau^{-1} = k_0 + A_1 \exp(-E_1^*/RT) + A_2 \exp(-E_2^*/RT) \quad (12)$$

The first Arrhenius term is the water quenching rate $k_{si} = A_1 \exp(-E_1^*/RT)$. If electron transfer is the only other temperature-dependent nonradiative process, the second Arrhenius term gives the electron transfer rate $k_{et} = A_2 \exp(-E_2^*/RT)$. If electron transfer is temperature independent, then the temperature-independent nonradiative rate k_0 is larger than that expected from eq 7, and $k_{et} = \Delta k_0$. There are three nonradiative processes in the −100° rotamer: intersystem crossing, which is temperature independent, water quenching, and electron transfer. Fluorescence decays of the *cis*-W3 zwitterion in H_2O were measured at nine temperatures from 5 to 40 °C. The temperature data set was analyzed by two methods. Procedure I is a graphical method. Individual decay curves were fitted to biexponential functions as in eq 2, and an Arrhenius plot of $\ln(\tau_1^{-1} - k_0 - k_{si})$ versus $1/T$ was constructed. The k_0 value of $1.0 \times 10^8\ s^{-1}$ was estimated from eq 7 using the radiative rate k_r of *cis*-W3 in Table 1 and the intersystem crossing rate of tryptophan $k_{isc} = 5 \times 10^7\ s^{-1}$.[16] The water quenching rate k_{si} of NATA with $A_1 = 6 \times 10^{16}\ s^{-1}$ and $E_1^* = 12.6$ kcal/mol was also used.[16] Values of the frequency factor $A_2 = 3.9 \times 10^{13}\ s^{-1}$ and activation energy $E_2^* = 7.3$ kcal/mol for excited-state electron transfer are determined from the intercept and slope of the straight line, giving an electron transfer rate at 25 °C of $k_{et} = 1.7 \times 10^8\ s^{-1}$.

Table 3. Arrhenius Parameters

k_0 ($10^7\ s^{-1}$)	A_1 (s^{-1})	E_1^* (kcal/mol)	k_{si}[a] ($10^7\ s^{-1}$)	A_2 (s^{-1})	E_2^* (kcal/mol)	k_{et}[a] ($10^7\ s^{-1}$)	χ_r^2
cis-W3 zwitterion[b]							
14	1.0×10^{16}	10.6	17				4.0
9.2	1.6×10^{17}	12.9	5.5	5.8×10^{12}	6.1	20	3.3
				3.9×10^{13}[c]	7.3[c]	17	
cis-W3 anion[b]							
8.1	5.1×10^{17}	13.5	6.5				2.0
7.0	1.1×10^{17}	12.7	5.4	1.9×10^{12}	6.6	2.8	1.7
NATA[d]							
9.8	6.0×10^{16}	12.6	3.4	4.5×10^{10}	3.2	20	
cis-2-(3-indolyl) cyclcohexaneol[b]							
6.8	1.2×10^{17}	12.8	5.0				1.7
3-methylindole[d]							
6.0	1.2×10^{17}	12.7	5.9				

[a] 25 °C. [b] Emission wavelength 370 nm. [c] Determined by Procedure I. [d] Reference 16.

Procedure II is a global analysis of the temperature data set. The short lifetime component of the *cis*-W3 zwitterion represents <2% of the steady-state intensity, so the decay curves were fitted to a single-exponential function as in eq 6. Decay curves at different temperatures were deconvolved in a multiple curve analysis with k_0, A_i, and E_i^* constrained to be the same in all of the curves. The fit assuming a single Arrhenius term gave $\chi_r^2 = 4.0$. The fit assuming two Arrhenius terms improved somewhat to $\chi_r^2 = 3.3$ with $k_0 = 9.2 \times 10^7\ s^{-1}$, $A_1 = 1.6 \times 10^{17}\ s^{-1}$, $E_1^* = 12.9$ kcal/mol, $A_2 = 5.8 \times 10^{12}\ s^{-1}$, and $E_2^* = 6.1$ kcal/mol. The electron transfer rate at 25 °C calculated from A_2 and E_2^* is $k_{et} = 2.0 \times 10^8\ s^{-1}$. The Arrhenius parameters A_1 and E_1^* determined for water quenching in *cis*-W3 are slightly higher than the values in NATA (Table 3). The Arrhenius parameters for excited-state electron transfer A_2 and E_2^* obtained by Procedures I and II agree reasonably well. The activation energies in *cis*-W3 are about twice the value in NATA, though the electron-transfer rates at 25 °C for *cis*-W3 and NATA are the same.

Deprotonation of the ammonium reduces the electron transfer rate in the *cis*-W3 anion to barely detectable levels. Using eqs 1 and 3 to estimate k_{et} as above gives $k_{et} = 2.1 \times 10^7\ s^{-1}$. The temperature dependence of the fluorescence lifetime of the *cis*-W3 anion in H_2O was measured at seven temperatures from 5 to 55 °C. Global analysis of the temperature data set according to eq 6 gave $\chi_r^2 = 2.0$ for a single Arrhenius term, which improved slightly to $\chi_r^2 = 1.7$ for two Arrhenius terms. The electron transfer rate at 25 °C calculated from A_2 and E_2^* is $k_{et} = 2.8 \times 10^7\ s^{-1}$. The slower electron-transfer rate in the *cis*-W3 anion as compared to the zwitterion is consistent with the proposition that the electrophilicity of carboxyl is enhanced by the adjacent positively charged amine.[10] The water quenching

rate at 25 °C calculated from A_1 and E_1* is $k_{si} = 5.4 \times 10^7$ s^{-1}, the same as in the zwitterion. The temperature dependence of the lifetime of *cis*-2-(3-indolyl)cyclohexanol in H_2O was measured at eight temperatures from 5 to 60 °C. Global analysis gave an acceptable χ_r^2 value for a single Arrhenius term. The water quenching rate is $k_{si} = 5.0 \times 10^7$ s^{-1}. The presence of the cyclohexyl ring does not appear to affect the water quenching rate. The k_{si} values for *cis*-W3, *cis*-2-(3-indolyl)cyclohexanol, and 3-methylindole are about the same, although larger than the value for NATA.

Conclusions

In this paper, we design a constrained tryptophan that provides a definitive test of the rotamer model for tryptophan photophysics in an aqueous environment. We also identify the intramolecular quenching mechanisms and measure the rates of excited-state proton and electron transfer in individual ground-state rotamers. The conformational constraint in *cis*-W3 eliminates rotation about the $C_\alpha - C_\beta$ bond of the tryptophan side chain and puts the amino and carboxyl groups at precise positions that mimic the $\chi_1 = 60°$ rotamer of tryptophan. The electronic properties of the indole ring are preserved, as the absorption spectra of *cis*-W3 and tryptophan are identical. The simulated and experimental time constants for relaxation of water around excited tryptophan are 1−2 ps,[43,44] so the biexponential fluorescence decay of *cis*-W3 cannot be due to solvent relaxation. X-ray crystallography shows a single $\chi_2 = -90°$ rotamer of *cis*-W3. Molecular mechanics calculations support two χ_2 rotamers in solution, −100° and 80°. The calculated χ_2 rotamer populations match the relative amplitudes of the two fluorescence lifetime components, assigning the major component with the longer lifetime to the $\chi_2 = -100°$ rotamer. Fluorescence decay times represent lifetimes of individual ground-state conformations only if the conformers do not interconvert in the excited state. We may estimate the rotamer interconversion rate $k_{rot1\rightarrow rot2}$ by transition-state theory

$$k_{rot1\rightarrow rot2} = \kappa(kT/h)\exp(-\Delta G^{\ddagger}/RT) \qquad (13)$$

where κ is the transmission coefficient, k is the Boltzmann constant, and h is the Planck constant. Assuming $\kappa = 1$ and $\Delta G^{\ddagger} = \Delta H^{\ddagger}$ and using the calculated enthalpy barrier of 7.6 kcal/mol from $\chi_2 = 80°$ to $\chi_2 = -100°$, $k_{80°\rightarrow -100°} = 1.7 \times 10^7$ s^{-1}, which is slower than any of the decay rates. The conversion rate from $\chi_2 = -100°$ to $\chi_2 = 80°$ is even slower, $k_{-100°\rightarrow 80°} = 2.6 \times 10^6$ s^{-1}. Because these estimated rates are likely upper limits,[45] we assume that χ_2 rotamer interconversion has a negligible effect on the fluorescence decay kinetics. However, these interconversion rates are fast as compared to the NMR time scale, so the two conformers in fast exchange have only a single set of resonances.[32]

The carboxyl group does not quench 3-methylindole fluorescence intermolecularly[16,46] or intramolecularly in indole-3-alkanoic acids[47] unless it is protonated. Fleming and co-workers proposed that the electrophilicity of carboxylate is enhanced in the tryptophan zwitterion by the adjacent ammonium.[10,11] Our results support their proposed mechanism and provide a value of about 2×10^8 s^{-1} at 25 °C for k_{et} in the $\chi_2 = -100°$ rotamer of the *cis*-W3 zwitterion. Electron transfer rates depend on the distance between donor and acceptor.[48] In the two χ_2 rotamers, the through-bond distances between indole and carboxylate are identical, and the through-space distances are nearly so. Thus, the k_{et} values should be about the same for both rotamers, whether electron transfer occurs through-bond or through-space. The dominant fluorescence quenching mechanism in the major −100° rotamer is excited-state electron transfer to carboxylate. However, the proton transfer rate k_{pt} in the minor 80° rotamer is an order of magnitude faster than k_{et}. Electron transfer is also a quenching mechanism in the 80° rotamer, but the dominant quenching mechanism is regioselective excited-state proton transfer at C5. Intramolecular proton transfer does not occur at C8 in the major −100° rotamer of *cis*-W3, despite similar N2···C5 and N2···C8 distances in the 80° and −100° rotamers. The criteria for proton transfer at a given position are not apparent from photochemical H−D exchange data or ab initio calculations on indole derivatives. Intramolecular proton transfer was likewise observed at the C4 position, but not at the C2 position in the tryptophan zwitterion.[9] However, glycine-catalyzed intermolecular proton transfer in 2- and 3-methylindoles was more extensive at the unsubstituted position of the pyrrole ring than at the C4 and C7 positions of the benzene ring.[14] The C3 loses π-electron density in the ^1L_a state of indole, while C2 gains less density than C4 and C7.[49] Perhaps, stringent geometric requirements for the formation of the proposed tetrahedral transition state in proton exchange preclude intramolecular proton transfer in the pyrrole ring of *cis*-W3 and tryptophan.

The two fluorescence lifetimes of the *cis*-W3 zwitterion are very close to those of tryptophan. It is tempting to speculate, by analogy with *cis*-W3, that excited-state electron transfer is responsible for the longer lifetime of tryptophan. The shorter lifetime includes both excited-state proton and electron transfer with regioselective proton transfer at C4 being the dominant quenching mechanism. Excited-state proton transfer is unlikely to occur in the two $\chi_1 = 180°$ rotamers, because the amino group is far from the indole ring. However, the $\chi_1 = \pm 60°$ rotamers bring the amino group close to the indole ring, and one χ_2 rotamer of each χ_1 rotamer has the amino group close to C4.

The two fluorescence lifetimes of *cis*-*N*-acetyl-W3 cannot be so neatly explained by the rotamer model. Nevertheless, we argue that the observed lifetime heterogeneity is probably rooted in ground-state heterogeneity as well. First, the low calculated enthalpy barriers between $\phi = 60°$ and −45° conformers predict rapid interconversion of ϕ conformers at rates of $0.4-1.6 \times 10^9$ s^{-1}. This confounds simple interpretation of fluorescence decay parameters in terms of populations and lifetimes of ground-state conformers. Conformer interconversion on the fluorescence time scale may produce lifetime heterogeneity even in the absence of a lifetime difference among conformers.[50] Second, the two intramolecular quenching mechanisms in *cis*-W3, excited-state electron transfer to carboxylate and proton

(43) Simonson, T.; Wong, C. F.; Brünger, A. T. *J. Phys. Chem. A* **1997**, *101*, 1935−1945.
(44) Shen, X.; Knutson, J. R. *J. Phys. Chem. B* **2001**, *105*, 6260−6265.
(45) Colucci, W. J.; Tilstra, L.; Sattler, M. C.; Fronczek, F. R.; Barkley, M. D. *J. Am. Chem. Soc.* **1990**, *112*, 9182−9190.
(46) Ricci, R. W.; Nesta, J. M. *J. Phys. Chem.* **1976**, *80*, 974−980.
(47) James, D. R.; Ware, W. R. *J. Phys. Chem.* **1985**, *89*, 5450−5458.
(48) Marcus, R. A.; Sutin, N. *Biochim. Biophys. Acta* **1985**, *811*, 265−322.
(49) Hahn, D. K.; Callis, P. R. *J. Phys. Chem. A* **1997**, *101*, 2686−2691.
(50) McMahon, L. P.; Yu, H.-T.; Shui, L.; Fronczek, F. R.; McLaughlin, M. L.; Barkley, M. D. *J. Phys. Chem. B* **1997**, *101*, 3269−3280.
(51) Gudgin, E.; Lopez-Delgado, R.; Ware, W. R. *J. Phys. Chem.* **1983**, *87*, 1559−1565.

transfer at C5, are eliminated by *N*-acetylation of the amino group. However, electron transfer to the amide bond is expected to be a quenching mechanism in *cis*-*N*-acetyl-W3.[16] The through-bond distances between indole and the amide group of *cis*-*N*-acetyl-W3 are the same in all conformations. On the other hand, the through-space distances are shorter, and the π-orbital overlap of the indole ring and the amide bond is better in both of the $\phi = -45°$ conformers than in the $\phi = 60°$ conformers. Through-space electron transfer would be faster in the $\phi = -45°$ conformers, shortening the fluorescence lifetime of the $\phi = -45°$ conformers relative to the $\phi = 60°$ conformers. The stable $\phi = 60°$ conformers of *cis*-*N*-acetyl-W3 are caused by the cyclohexane ring, as they are not found in the $\chi_1 = 60°$ rotamer of *N*-acetyltryptophan. This conformational constraint may account for the long fluorescence lifetime component observed in *cis*-*N*-acetyl-W3.

Acknowledgment. This work was supported by NIH grant GM42101.

Supporting Information Available: Table of crystal data, structure solution and refinement, atomic coordinates, bond lengths and angles, and anisotropic thermal parameters in CIF format. This material is available free of charge via the Internet at http://pubs.acs.org.

JA016542D